

Hong-Zhong HUANG  
Kang YU  
Tudi HUANG  
He LI  
Hua-Ming QIAN

## RELIABILITY ESTIMATION FOR MOMENTUM WHEEL BEARINGS CONSIDERING FRICTIONAL HEAT

### OCENA NIEZAWODNOŚCI ŁOŻYSK KÓŁ ZAMACHOWYCH Z UWZGLĘDNIENIEM CIEPŁA TARCIA

*Momentum wheels are the key components of the inertial actuators in the satellites, and the momentum wheel bearings are weak links of momentum wheels as they operate under harsh conditions. The reliability estimation for momentum wheel bearings are helpful to guarantee the mission successes for both momentum wheels and satellites. Hence, this paper put emphasis into reliability estimation of a momentum wheel bearing considering multiple coupling operating conditions and frictional heat by using the finite element analysis. The stress-strength interference model is employed to calculate the reliability of the momentum wheel bearing. A comparative analysis for reliability estimation with and without frictional heat of the momentum wheel bearing is conducted. The results show that the frictional heat cannot be ignored in the reliability analysis of momentum wheel bearings.*

**Keywords:** Momentum wheel bearings, Finite element analysis, Frictional heat, Stress-strength interference model.

*Kola zamachowe są kluczowymi elementami składowymi silowników bezwładnościowych w satelitach. Ich łożyska stanowią słaby punkt podczas pracy w trudnych warunkach. Ocena niezawodności łożysk kół zamachowych pozwala zapewnić powodzenie misji zarówno w odniesieniu do samych kół zamachowych, jak i satelitów. Dlatego też niniejszy artykuł poświęcono zagadnieniu oceny niezawodności łożyska koła zamachowego z wykorzystaniem analizy metodą elementów skończonych przy uwzględnieniu wielu sprzężonych warunków pracy oraz ciepła tarcia. Do obliczenia niezawodności łożyska koła zamachowego zastosowano model obciążeniowo-wytrzymałościowy. Przeprowadzono także analizę porównawczą oceny niezawodności łożyska koła zamachowego z uwzględnieniem lub bez uwzględnienia ciepła tarcia. Wyniki pokazują, że w analizie niezawodności łożysk kół zamachowych nie można pominąć ciepła tarcia.*

**Słowa kluczowe:** łożyska kół zamachowych, analiza MES, ciepło tarcia, model obciążeniowo-wytrzymałościowy.

#### Acronyms and Abbreviations

FEA	Finite element analysis
MW	Momentum wheel
MWB	Momentum wheel bearing
PDF	Probability distribution function
SSI	Stress-strength interference

#### Notations

$N(\cdot)$	Normal distribution
$P(\cdot)$	Probability for a random variable
$R(\cdot)$	Reliability
$s$	Stress
$\sigma$	Strength
$f_s(x)$	PDF of the stress
$f_\sigma(x)$	PDF of the strength
$\Phi(\cdot)$	Standard normal cumulative distribution function

#### 1. Introduction

Momentum wheels (MWs) are used for changing orientation of satellites. With advantages of low-power consumption, strong anti-disturbance ability, contamination-free and high-control precision, MWs have been widely adopted in attitude and orbit control system of satellites. However, the failure of MWs frequently occurred, according to the observation data from [33]. On the one hand, the failure of MWs will lead to catastrophic consequences to inertial actuators, even to the whole satellites [5]. On the other hand, the attitude control of satellites relies on MWs. Hence, the reliability estimation for MWs is essential to guarantee high reliability and mission success of satellites [4].

Due to the limitations of cost, time and difficulties in data collection, reliability estimation of MWs is always restricted by small amount data [22, 18, 21, 35]. To this end, the reliability estimation of MWs mainly relies on the simulation, testing and degradation models [3, 12, 19, 27, 28, 30]. The Russian Academy of Science adopted degradation based method and related testing technology to estimate the lifetime of the turned gyroscope RBHK05-78, and a remaining useful life of 30000 hours was estimated by using the extrapolation method [10]. The venerable companies, BENDIX of USA and TELDIX of German, led the research of MWs. To test the reliability of permanent

magnetic rate integrating gyroscopes, BENDIX took 326 products as samples and spent 794240 hours. TELDIX has provided 588 momentum wheels for 235 satellites, and the total no-failure on-orbit time is up to 2200 years [13]. Jin [9] proposed a method based on the relationship between the MWs' physical performances and their failure mechanisms to evaluate the reliability of MWs. In this method, a stochastic threshold Gauss-Brown process model was put forward to describe the failure process of MWs. Liu [23] and Jin [8] introduced Bayesian method to fuse multi-source information to carry out reliability assessment of MWs. According to engineering practice and testing results, the reliability of MWs relies on the high reliability and long usage life of momentum wheel bearings (MWBs), which are weak links of MWs. From field collection point of view, failures of MWBs occupied the first place in the failures of MWs [31, 32]. The methods of estimating the reliability of WMs often cost a lot of time and money currently. Though reliability estimation on bearings is widely conducted under certain working condition [6, 7, 11, 14, 15, 21, 29, 37, 38], the method of estimating the reliability of MWBs under working condition based finite element analysis (FEA) is rare. Furthermore, this paper takes frictional heat into consideration by adopting the FEA and stress-strength interference (SSI) model to evaluate the reliability of the target MWB. A comparative analysis was conducted, which indicates that the reliability of the MW is relatively affected by the frictional heat. A method based on FEA and SSI model is introduced here, which provides a solution to the reliability estimation for the small sample size products.

The rest of this paper is organized as follows. The finite element analysis of the MWB is carried out in section 2. Section 3 introduces the SSI model. SSI based reliability estimation for the MWB of the MW is conducted in Section 4. Section 5 provides the conclusions of this research.

## 2. Finite Element Analysis

### 2.1. Introduction of the MWB

This paper analyzes a MWB of a real MW equipped in a satellite of China. The MWB is a deep groove ball bearing with an inner ring, an outer ring, eight rolling elements and a cage.

The software namely SOLIDWORKS is used to build the three dimensional model of the MWB, and ANSYS WORKBENCH is employed to carry out FEA. The three dimensional model is shown in Fig. 1 and each MWB consists of inner ring, outer ring, cage and 8 rolling elements. The main parameters of the MWB are listed in Table 1.

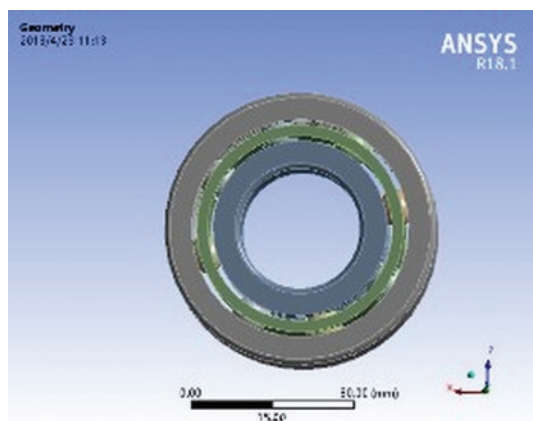


Fig. 1. Three dimensional model of the MWB

Table 1. The main parameters of the MWB

Parameter	value	Parameter	value
Bearing outside diameter (mm)	50	Number of balls	8
Bearing bore diameter (mm)	22	Rib diameter of outer ring (mm)	40
Bearing width (mm)	14	Rib diameter of inner ring (mm)	32
Ball diameter (mm)	7		

The MWB was made by GCr15, which has great performance on corrosion resistance and high strength. The density (7830kg/m<sup>3</sup>), Poisson's ratio (0.3) and coefficient of linear expansion (1.25e-5/°C) of GCr15 are regarded as constant in this study. The changes of elasticity modulus and thermal conductivity of GCr15 together with temperature are shown in Table 2.

Table 2. Material properties of GCr15 changing along with time

Temperature $T/^\circ\text{C}$	Elasticity modulus $E/\text{GPa}$	Thermal conductivity $k/W/(m\cdot^\circ\text{C})$
20	200	40.1
200	192	37.85
400	175	34.5
600	153	30.1

### 2.2. Static-structure Analysis

Contact pairs are automatically generated when the model of MWB is imported into the ANSYS WORKBENCH. The model of the MWB has 8 rolling elements and 24 pairs of contact. Taking the surfaces of cage holes and raceway's groove surfaces of the inner ring and the outer ring as target surfaces, and taking the sphere surfaces of balls as contact surfaces, 24 pairs in total of contact are built in the analysis. All of the contact types are defined as frictional contact with the friction coefficient 0.02.

Meshing of the finite element analysis affects the results directly. Meshing is related to both accuracy of analysis results and calculation time. This paper takes these both parameters into consideration. Moreover, a module named Mesh Quality Check is applied to ensure the quality of the meshing element. The meshing of the MWB creates 10084 elements and 29739 nodes, as shown in Fig. 2.

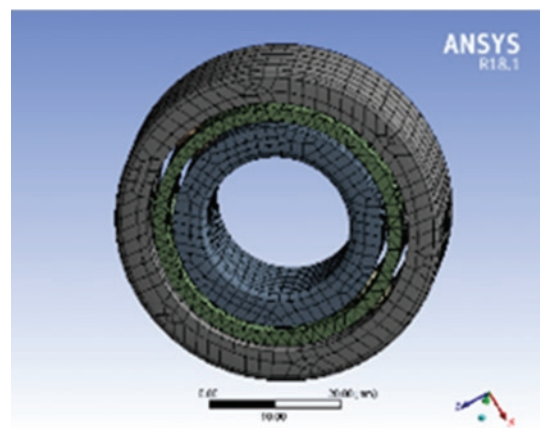


Fig. 2. The meshing of the bearing

**Loads and boundary conditions**

The inner ring of MWB is fixed to the shaft while the outer ring revolves around the axis.

- 1) To simulate the assemblage of the inner ring and the shaft, a fixed support constraint is applied to the inner surface of the inner ring.
- 2) To simulate the role of the sleeve bearing, axial displacement constraints are applied to end surfaces of the outer ring, the inner ring and the cage.
- 3) To simulate the rotation and the assemblage of the outer ring, a rotational velocity is applied to the whole outer ring around the axial orientation, and a radial force, which points into inside, is applied to the outside surface of the outer ring.

**Static structure analysis result**

In static structure analysis module, equivalent stress is added in the solution to detect the stress of the riskiest point on the MWB. Fig. 3 shows the results of the equivalent stress of the MWB when the rotation velocity of the outer ring is 10000 rpm, and the radial force of the outer ring is 1200 N. The maximum stress points of the inner ring, outer ring and cage of the appeared at the position of contact with the rolling elements. The maximum stress on different parts of the MWB are listed in Table 3.

As shown in Table 3 and Fig. 3, the maximum stress is on the rolling element, more specifically, the contact region of the ball and the outer ring. The maximum stress is 368.61MPa, which is regarded as the riskiest point. The second maximum stress part of the MWB is the inner ring, amounting to 305.98MPa. The third maximum part is

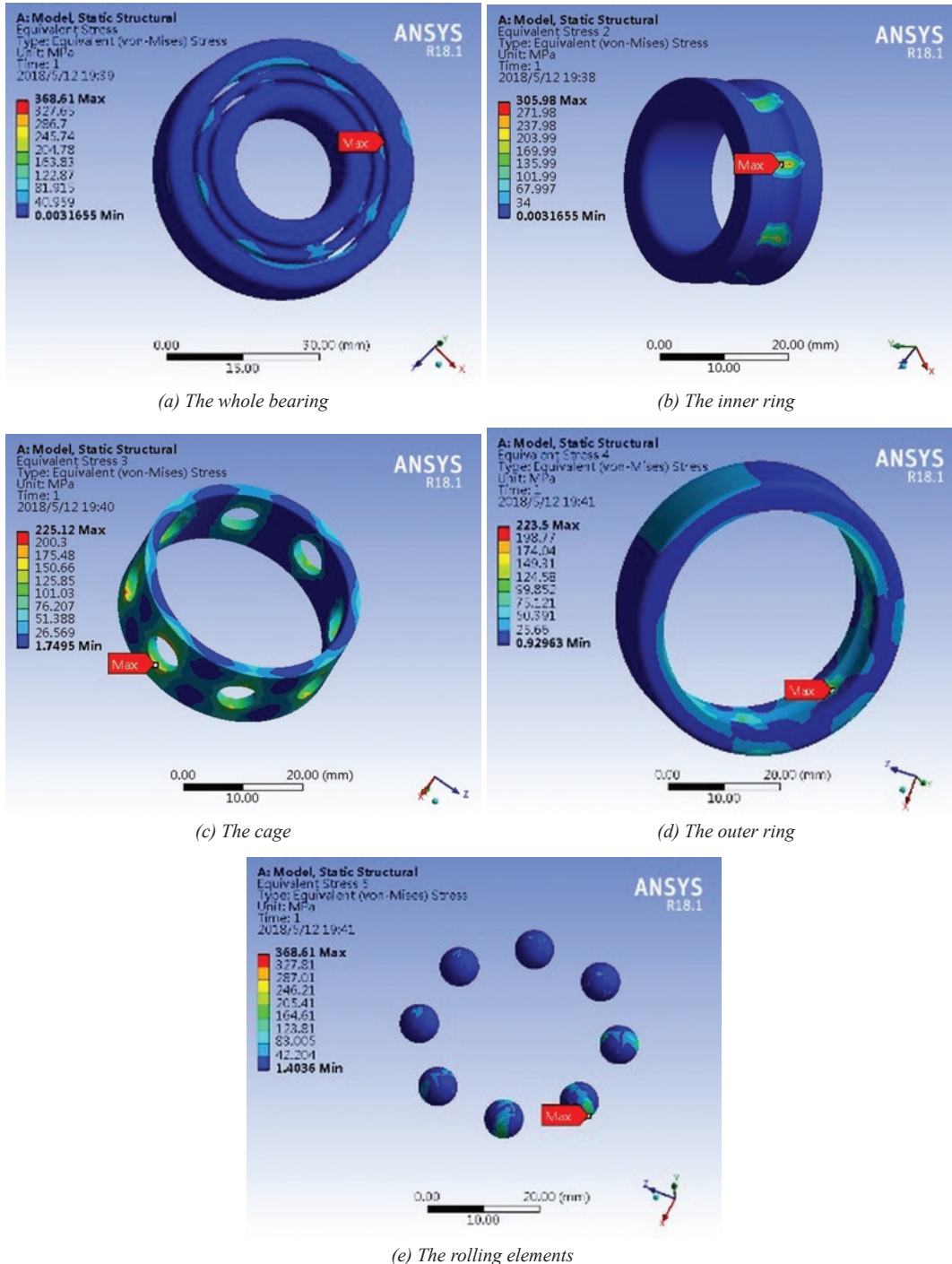


Fig. 3. Static structure analysis results

Table 3. The maximum stress on different parts of the MWB

Different part of the MWB	The maximum stress (MPa)	Different part of the MWB	The maximum stress (MPa)
The inner ring	305.98	The outer ring	225.12
The cage	223.50	The rolling elements	368.61

of the cage, amounting to 225.12MPa. The minimum stress part is the outer ring, amounting to 223.5MPa. The result in Table 3 is accordance with factual reality, which indicates the correctness of the FEA in this paper.

2.3. FEA of the MWB Considering Frictional Heat

The MWB produces frictional heat between the rolling elements and inner ring, the outer ring and cage. The friction may influence the stress of the riskiest point of the MWB. To this end, this paper adopted indirect coupling method in FEA. Steady-state thermal analysis is firstly completed, then the result is imported to static structure analysis as a thermal load.

Finally, the thermal-mechanical FEA is accomplished.

Steady-state thermal analysis

- (1) According to the installation and working conditions of MWB, the Loads and boundary conditions are shown as follows:

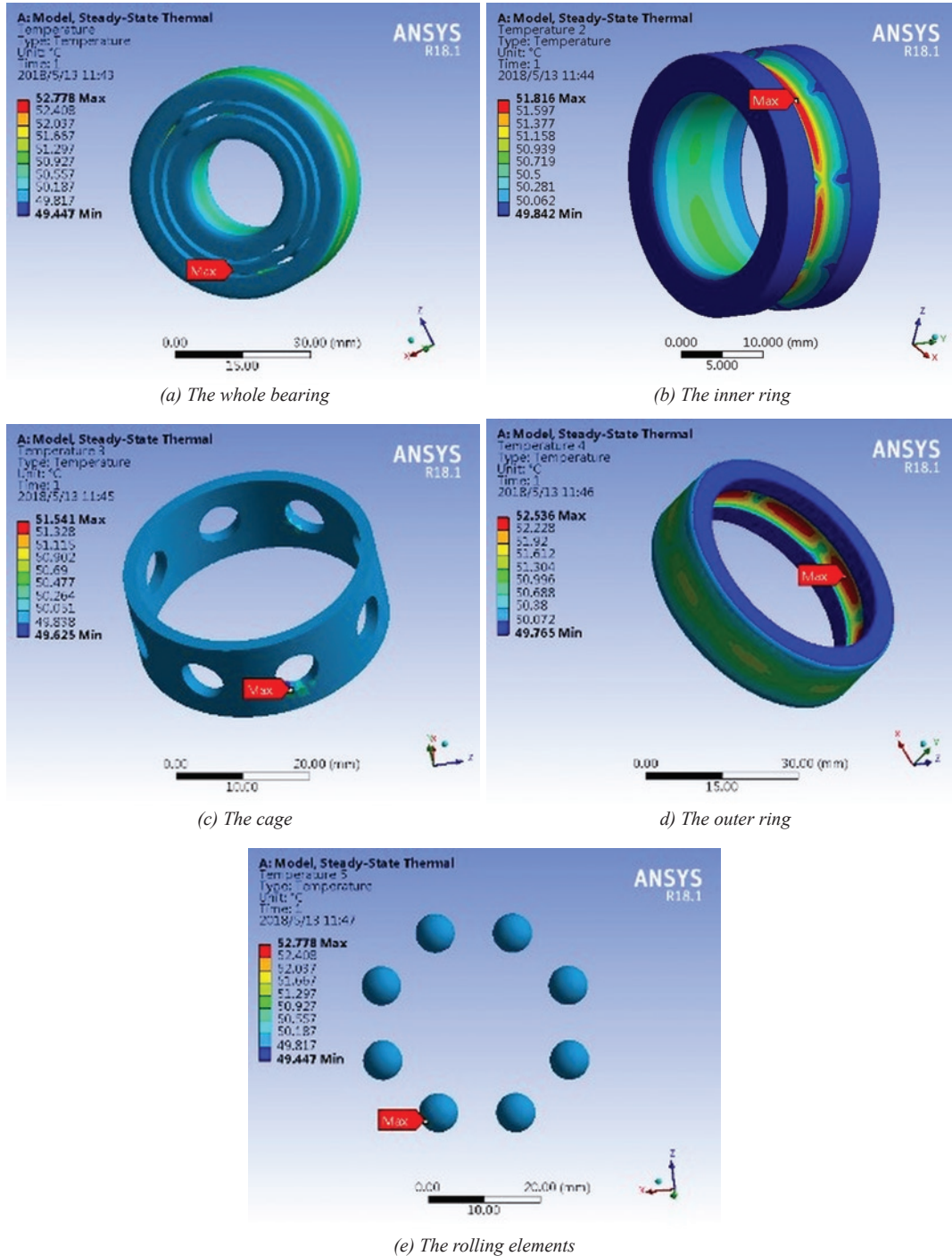


Fig. 4. The steady-state thermal analysis results

- 1) The heat generated by the friction between the rolling elements and the raceways is loaded in the form of heat flux to the raceway surfaces, which is 42W.
- 2) The heat generated by the friction between the rolling elements and the cage is applied in the form of heat flux to the hole surfaces of the cage, which is 5W.
- 3) Applied the convection to the outer surfaces of the inner ring, outer ring and the body surface, which is  $60 \text{ W} / (\text{mm}^2 \cdot ^\circ\text{C})$ .
- (2) The results of steady-state thermal analysis of different parts of the WMB are shown in Fig. 4.

From Fig. 4, the highest temperature of the inner ring, outer ring and retainer appears at the position of contact with the rolling elements. And the highest temperature is  $52.778^\circ\text{C}$ , which locates on the rolling element, specifically, the contact area between the ball and the

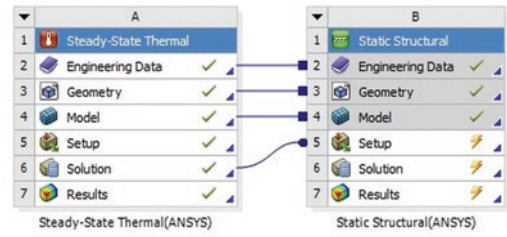


Fig. 5. The process of thermal-mechanical coupling analysis

outer ring. The second highest temperature part of the MWB is the outer ring, amounting to  $52.536^\circ\text{C}$ . The third highest temperature part

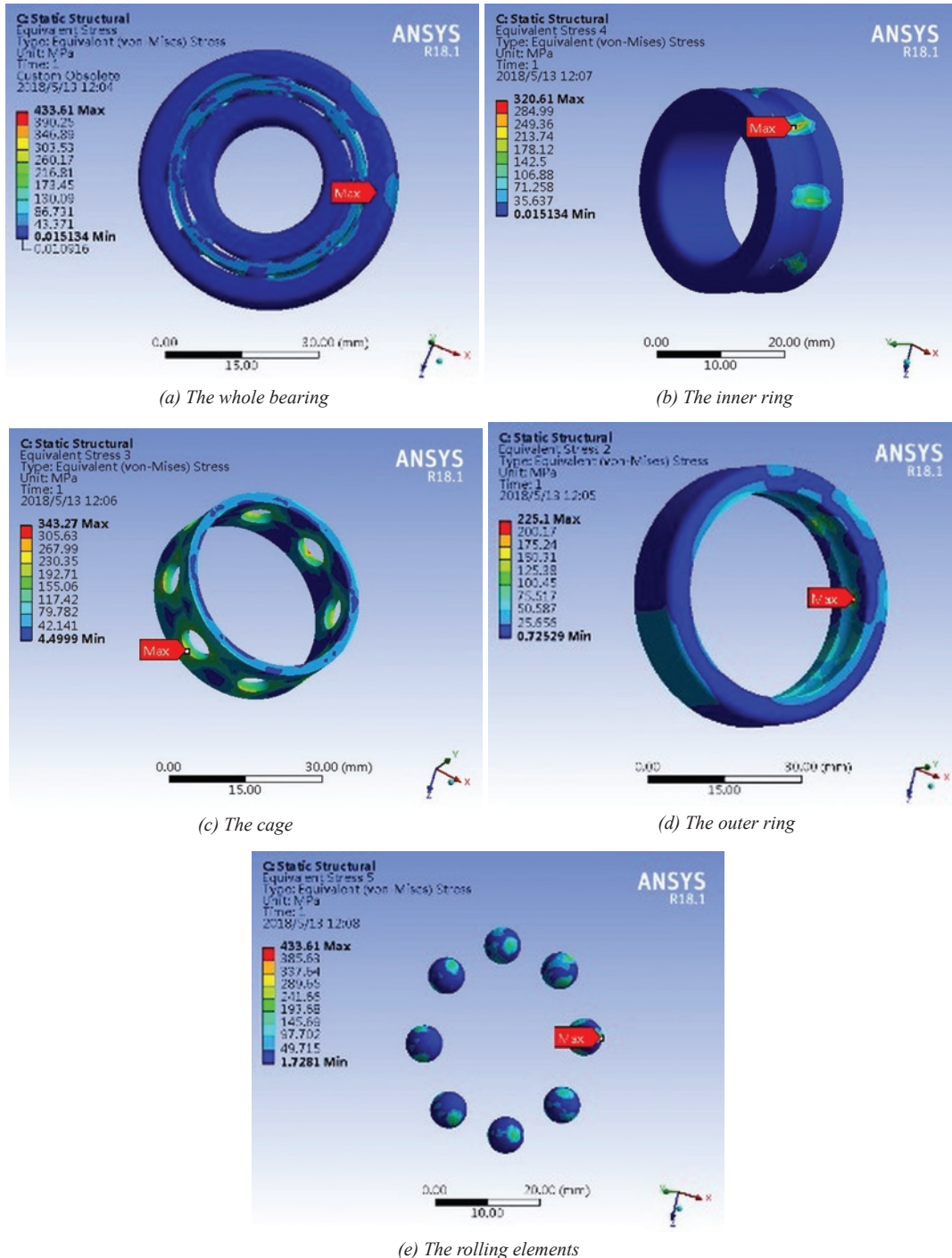


Fig. 6. The results of thermal-mechanical coupling FEA

of the MWB is inner ring, amounting to 51.816°C. The fourth highest temperature part of the MWB is cage, amounting to 51.541°C.

**Thermal-mechanical coupling analysis**

This paper considers both efficiency of calculation and working conditions of the MWB. The process is shown in Fig. 5.

The result of steady-state thermal analysis is imported into the static-structure analysis as the thermal load. Other loads and boundary conditions are same to the static-structure analysis. The results of thermal-mechanical coupling FEA are shown in Fig. 6.

It can be seen from Fig. 6 that the maximum stress is up to 433.61MPa located on the contact area between the rolling elements and the outer ring. It is evident that the stress on the WMB increases considerably due to the frictional heat, which indicates that the thermal field cannot be ignored when undertaking FEA to the MWB. That is to say the reliability estimation result is more accurate when taking frictional heat into consideration than not. It is shown in Fig. 6 that the maximum stress is on the rolling element, more specifically, the contact region of the ball and the outer ring. The maximum stress is 433.61MPa, which is regarded as the riskiest point.

**3. Stress-Strength Interference Model**

Stress-strength interference (SSI) model has been widely used in the reliability estimation [1, 2, 25, 36]. In SSI model, Stress represents a number of factors promoting the failure while strength represents ability of resisting the failure of products. Products fail or not depends on the relationship between the stress and the strength. Failure occurs if the stress is larger than the strength, otherwise structures would be safe [16, 17, 20]. In practice, uncertainties exist in both stress and strength, thus stress and strength is no longer a constant value as most researchers did [34]. It is proper to describe them by distributions [24]. The reliability of a structure is defined as the probability of strength is larger than stress.

The probability density function (PDF) of strength is represented as  $f_s(y)$ , and the PDF of stress is represented as  $f_s(x)$ . According to the definition of the SSI model, the reliability of the structure is calculated by Eq. (1):

$$R = P(Y - X > 0) = \int_{-\infty}^{\infty} f_s(y) \left[ \int_{-\infty}^y f_s(x) dx \right] dy \quad (1)$$

If both X and Y follow normal distribution  $X \sim N(\mu_x, \sigma_x^2)$ ,  $Y \sim N(\mu_y, \sigma_y^2)$ , their proper function is  $Z = Y - X$ . According to the property of normal distribution, Z is also follow a normal distribution  $Z \sim N(\mu_z, \sigma_z^2)$ . Moreover,  $\mu_z = \mu_y - \mu_x$ ,  $\sigma_z = \sqrt{\sigma_x^2 + \sigma_y^2}$ . Then, Eq. (1) can be transformed to Eq. (2):

$$\begin{aligned} R &= P(Y - X > 0) \\ &= P(Z > 0) \\ &= \int_0^{\infty} \frac{1}{\sqrt{2\pi}\sigma_z} \exp\left[-\frac{1}{2}\left(\frac{Z-\mu_z}{\sigma_z}\right)^2\right] dZ \\ &= \Phi\left(\frac{Z-\mu_z}{\sigma_z}\right) \end{aligned} \quad (2)$$

**4. Reliability Estimation of MWB**

Owning to complex working conditions, the rotational velocity of the MWB is not a constant value but a distribution. The rotational speed of the bearing can be represented by a normal distribution with mean value of 10000 and standard deviation of 100, which means  $\omega \sim N(10000, 100^2)$  [7]. Taking 40 random numbers from the normal distribution of the rotational speed, and adopted them into FEA. In order to analyze the effect of frictional heat on the reliability of the MWB, both the static structure analysis and thermal-mechanical coupling analysis were undertaken 40 times under different rotational velocity. The stress on the riskiest point of the MWB were calculated by the FEA, as shown in Table 4.

In Table 4,  $n$  represents the rotational velocity of the outer ring,  $S_1$  and  $S_2$  represents the maximum stress of the bearing under the static structure analysis and thermal-mechanical analysis, respectively. The histograms of stress on the riskiest point of the MWB are shown in Fig. 7.

$S_1$  and  $S_2$  follow normal distributions, as presented in Fig. 8.

It is can be seen from Fig. 7, there are 40 simulation data in each of the two conditions. Therefore, the  $S_1$  and  $S_2$  can be fit by normal distribution. Then, Lilliefors test is taken, and the results show that  $S_1$  and  $S_2$  follow normal distribution well. The software of MATLAB was used to fit  $S_1$  and  $S_2$ , and the results are  $S_1 \sim N(370.6678, 7.7655^2)$  and  $S_2 \sim N(434.9405, 6.7781^2)$ .

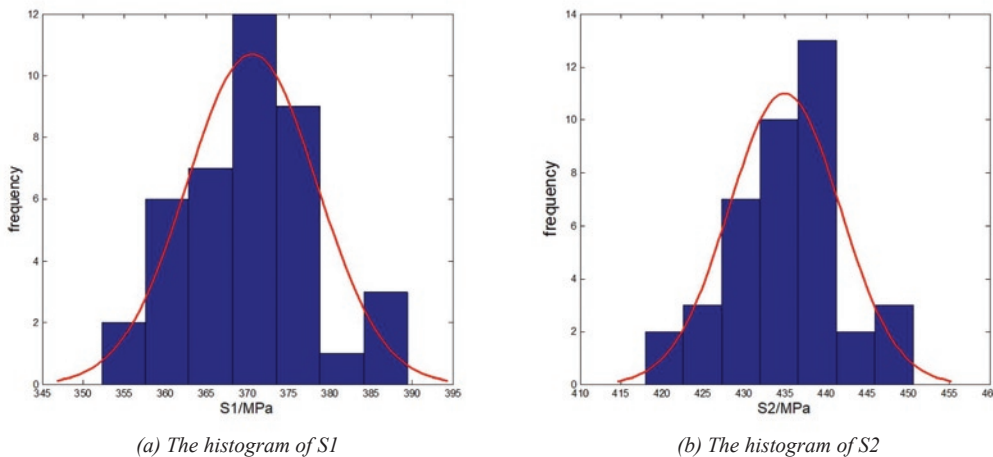


Fig.7. The histograms of stress on the riskiest point of the MWB

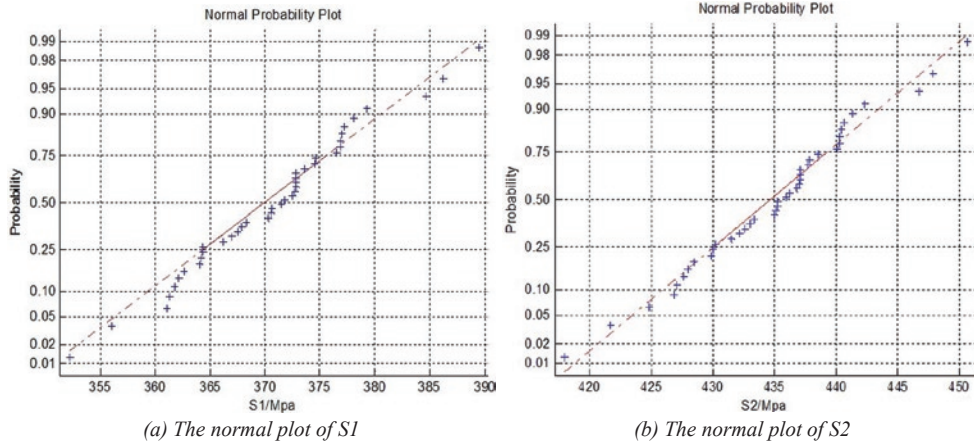


Fig. 8. The normal plot of the stress on the riskiest point of the MWB

Table 4. The stress on the riskiest point of the MWB at various rotational speed

$n/rpm$	$S_1/MPa$	$S_2/MPa$	$n/rpm$	$S_1/MPa$	$S_2/MPa$
10054	371.79	436.23	10072	372.78	437.06
10183	379.23	442.31	10163	378.07	441.34
9774	355.99	421.71	10049	371.45	435.96
10086	373.60	437.73	10103	374.59	438.50
10032	374.47	435.13	10073	372.83	437.10
9869	361.27	427.06	9970	366.94	432.15
9957	366.19	431.51	10029	370.30	434.99
10034	370.63	435.26	9921	364.15	429.97
10358	389.45	450.63	10089	372.82	437.87
10277	384.67	446.74	9885	362.17	427.97
9865	361.06	426.84	9893	362.60	428.40
10303	386.19	447.86	9919	364.04	429.86
10073	372.83	437.10	9706	352.25	417.96
9994	368.28	433.33	10144	376.96	440.42
10071	372.72	437.01	10033	370.57	435.22
9980	367.48	432.61	9925	364.36	430.18
9988	367.91	433.03	10137	376.52	440.08
10149	377.24	440.65	9829	359.05	424.80
10141	376.80	440.31	10067	372.50	436.83
10142	376.85	440.32	9879	361.80	427.59

Due to insufficient data of MWB, and the influence of manufacturing technology and assembly level, it is difficult to obtain the intensity distribution of MWB. In this paper, the intensity distribution of material is approximately used as the intensity distribution of MWB. The strength of GCr15 follows normal distribution  $\delta \sim N(518.42, 51.842^2)$ .

According to the SSI model, the reliability of the MWB can be calculated by Eq. (2):

$$R_1 = P(\delta - S_1 > 0) = \Phi\left(\frac{518.42 - 370.6678}{\sqrt{51.842^2 + 7.7655^2}}\right) = 0.99759$$

$$R_2 = P(\delta - S_2 > 0) = \Phi\left(\frac{518.42 - 434.9405}{\sqrt{51.842^2 + 6.7781^2}}\right) = 0.94483$$

$R_1$  and  $R_2$  represent the reliability of the MWB under the static-structure analysis and under the thermal-mechanical coupling analysis, respectively. The results indicate that frictional heat does affect the reliability of MWB, and frictional heat cannot be ignored in the reliability estimation of the MWB.

### 5. Conclusions

In this paper, a reliability estimation method for MWBs based on FEA and SSI model is proposed. Firstly, the thermal-mechanical coupling FEA to the MWB is carried out. Then, the reliability estimation based on stress-strength interference model and the comparison analysis between the static-structure analysis and the thermal-mechanical coupling analysis is fulfilled. The reliability under static-structure analysis is 0.99759, and the reliability under the thermal-mechanical

analysis is 0.94483. It is evident that the reliability decreases a lot owing to the effect of frictional heat, which indicates that the effect of frictional heat on the reliability of MWB cannot be ignored. Put it in another way, the reliability estimation result considering frictional heat proposed in this paper is more accurate than the method ignoring the frictional heat. Future work can be done by considering more

physical fields, for example, electrical field, magnetic field and so on to make the estimation result more close to practical engineering.

#### Acknowledgement

*This work was supported by the National Natural Science Foundation of China under contract No. 51875089.*

#### References

1. Al-Mutairi D K, Ghitany M E, Kundu D. Inferences on stress-strength reliability from Lindley distributions. *Communications in Statistics-Theory and Methods* 2013; 42(8): 1443-1463, <https://doi.org/10.1080/03610926.2011.563011>.
2. Bhuyan P, Dewanji A. Reliability computation under dynamic stress-strength modeling with cumulative stress and strength degradation. *Communications in Statistics-Simulation and Computation* 2017; 46(4): 2701-2713, <https://doi.org/10.1080/03610918.2015.1057288>.
3. Bingjie W, Guang J. Reliability modeling and analyzing of momentum wheel based on Gamma process. *Value Engineering* 2010; (1): 25-27.
4. Castet J F, Saleh J H. Beyond reliability, multi-state failure analysis of satellite subsystems: a statistical approach. *Reliability Engineering & System Safety* 2010; 95(4): 311-322, <https://doi.org/10.1016/j.res.2009.11.001>.
5. Castet J F, Saleh J H. Satellite and satellite subsystems reliability: Statistical data analysis and modeling. *Reliability Engineering & System Safety* 2009; 94(11): 1718-1728, <https://doi.org/10.1016/j.res.2009.05.004>.
6. Huang C G, Huang H Z, Li Y F. A Bi-Directional LSTM prognostics method under multiple operational conditions. *IEEE Transactions on Industrial Electronics* 2019; 66(11): 8792-8802, <https://doi.org/10.1109/TIE.2019.2891463>.
7. Jansen M J, Jones Jr W R, Pepper S V, Wheeler D R, Schroerer A, Fluehmann F, Shogrin B A. The effect of TiC coated balls and stress on the lubricant lifetime of a synthetic hydrocarbon (Pennzane 2001A) using a vacuum spiral orbit tribometer. In *Proceeding International Tribology Conference, Nagasaki, Japan; October 2000*.
8. Jin G, Feng J. Bayes-Weibull reliability assessment method for long life satellite moving components. *Systems Engineering and Electronics* 2009; 31(8): 2020-2023.
9. Jin G, Liu Q, Zhou J, Zhou Z. Repofe: Reliability physics of failure estimation based on stochastic performance degradation for the momentum wheel. *Engineering Failure Analysis* 2012; 22: 50-63, <https://doi.org/10.1016/j.engfailanal.2011.12.004>.
10. Jin G, Matthews D, Fan Y, Liu Q. Physics of failure-based degradation modeling and lifetime prediction of the momentum wheel in a dynamic covariate environment. *Engineering Failure Analysis* 2013; 28: 222-240, <https://doi.org/10.1016/j.engfailanal.2012.10.027>.
11. Khonsari M, Booser E R. Predicting lube life-heat and contaminants are the biggest enemies of bearing grease and oil. *Machinery Lubrication* 2003; 75(1): 89-90, 92.
12. Li H, Huang H Z, Li Y F, Zhou J, Mi J. Physics of failure-based reliability prediction of turbine blades using multi-source information fusion. *Applied Soft Computing* 2018; 72: 624-635, <https://doi.org/10.1016/j.asoc.2018.05.015>.
13. Li H, Pan D, Chen C L P. Reliability modeling and life estimation using an expectation maximization based wiener degradation model for momentum wheels. *IEEE transactions on cybernetics* 2014; 45(5): 969-977, <https://doi.org/10.1109/TCYB.2014.2341113>.
14. Li X Y, Huang H Z, Li Y F, Zio E. Reliability assessment of multi-state phased mission system with non-repairable multi-state components. *Applied Mathematical Modelling* 2018; 61: 181-199, <https://doi.org/10.1016/j.apm.2018.04.008>.
15. Li X Y, Li Y F, Huang H Z, Zio E. Reliability assessment of phased-mission systems under random shocks. *Reliability Engineering & System Safety* 2018; 180: 352-361, <https://doi.org/10.1016/j.res.2018.08.002>.
16. Li X, Huang H Z, Li F, Ren L. Remaining useful life prediction model of the space station. *Eksploatacja i Niezawodnos - Maintenance and Reliability* 2019; 21(3): 501-510, <https://doi.org/10.17531/ein.2019.3.17>.
17. Li X, Huang H Z, Li Y F, Li Y F. Reliability evaluation for VHF and UHF bands under different scenarios via propagation loss model. *Eksploatacja i Niezawodnos - Maintenance and Reliability* 2019; 21(3): 375-383, <https://doi.org/10.17531/ein.2019.3.3>.
18. Li Y F, Huang H Z, Liu Y, Xiao N, Li H. A new fault tree analysis method: fuzzy dynamic fault tree analysis. *Eksploatacja i Niezawodnos c-Maintenance and Reliability* 2012; 14(3): 208-214.
19. Li Y F, Huang H Z, Mi J, Peng W, Han X. Reliability analysis of multi-state systems with common cause failures based on Bayesian network and fuzzy probability. *Annals of Operations Research* 2019; <https://doi.org/10.1007/s10479-019-03247-6>, <https://doi.org/10.1007/s10479-019-03247-6>.
20. Li Y F, Mi J, Huang H Z, Xiao N C, Zhu S P. System reliability modeling and assessment for solar array drive assembly based on Bayesian networks. *Eksploatacja i Niezawodnos - Maintenance and Reliability* 2013; 15(2): 117-122.
21. Li Y F, Mi J, Huang H Z, Zhu S P, Xiao N. Fault tree analysis of train rear-end collision accident considering common cause failure. *Eksploatacja i Niezawodnos - Maintenance and Reliability* 2013; 15(4): 403-408.
22. Liu Q, Jin G, Zhou J. A modeling method of performance reliability of momentum wheel based on EMD. *Computer Simulation* 2007; 24(11): 32-34, 158.
23. Liu Q, Zhou J, Jin G, Li H T. Bayesian reliability estimation for momentum wheel based on credibility. *Journal of Astronautics* 2009; 30(1): 382-386.
24. Liu Y, Shi Y, Bai X, Liu B. Stress-strength reliability analysis of system with multiple types of components using survival signature. *Journal of Computational and Applied Mathematics* 2018; 342: 375-398, <https://doi.org/10.1016/j.cam.2018.04.029>.
25. Liu Y, Shi Y, Bai X, Zhan P. Reliability estimation of a NM-cold-standby redundancy system in a multicomponent stress-strength model with generalized half-logistic distribution. *Physica A: Statistical Mechanics and its Applications* 2018; 490: 231-249, <https://doi.org/10.1016/j.physa.2017.08.028>.
26. Masuko M, Mizuno H, Suzuki A, Obara S, Sasaki A. Lubrication performance of multi-alkylated cyclopentane oils for sliding friction of steel under vacuum condition. *Journal of Synthetic Lubrication* 2007; 24(4): 217-226, <https://doi.org/10.1002/jsl.41>.

27. Mi J, Li Y F, Peng W, Huang H Z. Reliability analysis of complex multi-state system with common cause failure based on evidential networks. *Reliability Engineering & System Safety* 2018; 174: 71-81, <https://doi.org/10.1016/j.ress.2018.02.021>.
28. Mi J, Li Y F, Yang Y J, Peng W, Huang H Z. Reliability assessment of complex electromechanical systems under epistemic uncertainty. *Reliability Engineering & System Safety* 2016; 152: 1-15, <https://doi.org/10.1016/j.ress.2016.02.003>.
29. Palladino M, Murer J, Didierjean S, Gaillard L. Life prediction of fluid lubricated space bearings: A case study. In *Proc. 14th Eur. Space Mechanisms Tribol. Symp* 2011; 279-285.
30. Prado J, Bisiacchi G, Reyes L, Vicente E, Contreras F, Mesinas M, Juares A. Three-axis air-bearing based platform for small satellite attitude determination and control simulation. *Journal of Applied Research and Technology* 2005; 3(3): 222-237.
31. Sathyan K, Gopinath K, Lee S H, Hsu H Y. Bearing retainer designs and retainer instability failures in spacecraft moving mechanical systems. *Tribology Transactions* 2012; 55(4): 503-511, <https://doi.org/10.1080/10402004.2012.675118>.
32. Sathyan K, Hsu H Y, Lee S H, Gopinath K. Long-term lubrication of momentum wheels used in spacecrafts-an overview. *Tribology International* 2010; 43(1-2): 259-267, <https://doi.org/10.1016/j.triboint.2009.05.033>.
33. Tafazoli M. A study of on-orbit spacecraft failures. *Acta Astronautica* 2009; 64(2-3): 195-205, <https://doi.org/10.1016/j.actaastro.2008.07.019>.
34. Wang B X, Geng Y, Zhou J X. Inference for the generalized exponential stress-strength model. *Applied Mathematical Modelling* 2018; 53: 267-275, <https://doi.org/10.1016/j.apm.2017.09.012>.
35. Xu H, Li W, Li M, Hu C, Zhang S, Wang X. Multidisciplinary robust design optimization based on time-varying sensitivity analysis. *Journal of Mechanical Science and Technology* 2018; 32(3): 1195-1207, <https://doi.org/10.1007/s12206-018-0223-8>.
36. Zhang J, Ma X, Zhao Y. A stress-strength time-varying correlation interference model for structural reliability analysis using copulas. *IEEE Transactions on Reliability* 2017; 66(2): 351-365, <https://doi.org/10.1109/TR.2017.2694459>.
37. Zhang X, Gao H, Huang H Z, Li Y F, Mi J. Dynamic reliability modeling for system analysis under complex load. *Reliability Engineering & System Safety* 2018; 180: 345-351, <https://doi.org/10.1016/j.ress.2018.07.025>.
38. Zheng B, Li Y F, Huang H Z. Intelligent fault recognition strategy based on adaptive optimized multiple centers. *Mechanical Systems and Signal Processing* 2018; 106: 526-536, <https://doi.org/10.1016/j.ymssp.2017.12.026>.

---

**Hong-Zhong HUANG**

**Kang YU**

**Tudi HUANG**

**He LI**

**Hua-Ming QIAN**

Center for System Reliability and Safety  
School of Mechanical and Electrical Engineering  
University of Electronic Science and Technology of China  
Chengdu, Sichuan, 611731, P. R. China

E-mails: hzhuang@uestc.edu.cn, yukang@std.uestc.edu.cn, huangtudi@std.uestc.edu.cn, heli@std.uestc.edu.cn, qianhuaming@std.uestc.edu.cn

---